Accepted Manuscript

Heparan Sulfate Proteoglycan Synthesis is Dysregulated in Human Osteoarthritic Cartilage

Anastasios Chanalaris, Hannah Clarke, Scott E. Guimond, Tonia L. Vincent, Jeremy E. Turnbull, Linda Troeberg

PII: S0002-9440(18)30512-1

DOI: https://doi.org/10.1016/j.ajpath.2018.11.011

Reference: AJPA 3053

To appear in: *The American Journal of Pathology*

Received Date: 16 June 2018

Revised Date: 6 November 2018

Accepted Date: 13 November 2018

Please cite this article as: Chanalaris A, Clarke H, Guimond SE, Vincent TL, Turnbull JE, Troeberg L, Heparan Sulfate Proteoglycan Synthesis is Dysregulated in Human Osteoarthritic Cartilage, *The American Journal of Pathology* (2019), doi: https://doi.org/10.1016/j.ajpath.2018.11.011.

Heparan Sulfate Proteoglycan Synthesis is Dysregulated in Human Osteoarthritic Cartilage

Anastasios Chanalaris[*], Hannah Clarke[†], Scott E. Guimond[†], Tonia L. Vincent[*], Jeremy E. Turnbull[†], Linda Troeberg[*]

[*] Arthritis Research UK Centre for Osteoarthritis Pathogenesis, Kennedy Institute of Rheumatology, University of Oxford, Roosevelt Drive, Oxford, OX3 7FY, UK

[†] Institute of Integrative Biology, University of Liverpool, Crown Street, Liverpool, L69 7ZB, UK

Number of text pages: 32; number of tables: 1 (+1 Supplementary); number of figures: 6.

Running title: Heparan sulfation altered in osteoarthritis

Funding: Supported by Arthritis Research UK grants 20887, 20205, and 21621 and the National Institute for Health Research (NIHR) Oxford Biomedical Research Centre (BRC).

Disclosures: The views expressed are those of the author(s) and not necessarily those of the NHS, the NIHR, or the Department of Health.

Address correspondence to: Linda Troeberg, Ph. D., Arthritis Research UK Centre for Osteoarthritis Pathogenesis, Kennedy Institute of Rheumatology, University of Oxford, Roosevelt Drive, Oxford, OX3 7FY, UK. E-mail: linda.troeberg@kennedy.ox.ac.uk

Abstract

Osteoarthritis (OA) is a common degenerative joint disease, characterized by cartilage loss and subchondral bone remodelling in response to abnormal mechanical load. Heparan sulfate (HS) proteoglycans bind to many proteins that regulate cartilage homeostasis, including growth factors, morphogens, proteases, and their inhibitors, and modulate their localization, retention, and biological activity. Changes in HS expression and structure may thus have important consequences for joint health. We analyzed normal and osteoarthritic human knee cartilage, and found HS biosynthesis was markedly disrupted in OA, with 45% of the 38 genes analyzed differentially regulated in diseased cartilage. The expression of several HS core proteins, biosynthesis, and modification enzymes was increased in OA cartilage, whereas the expression of the HS proteoglycans syndecan 4 and betaglycan was reduced. The structure of HS was also altered, with increased levels of 6-O-sulfation in osteoarthritic samples, which correlated with increased expression of *HS6ST1*, a 6-O-sulfotransferase, and *GLCE*, an epimerase that promotes 6-O-sulfation. siRNA silencing of *HS6ST1* expression in primary OA chondrocytes inhibited ERK phosphorylation in response to FGF2, showing that changes in 6-O-sulfation impact a key cartilage signalling pathway. Given the broad range of homeostatic and repair pathways that HS regulates, these changes in proteoglycan expression and HS structure are likely to have significant effects on joint health and progression of OA.

Introduction

Osteoarthritis (OA) is a common degenerative joint disease in which articular cartilage loss and subchondral bone remodelling cause pain and impair movement of affected joints. There are currently no disease-modifying therapies available, and patients are largely treated with analgesia or joint replacement surgery. There is thus a substantial need to develop effective therapeutics that can slow or halt the progression of joint damage.

The primary risk factors for development of OA are ageing and injury, which alter the mechanical environment of the joint and stimulate chondrocytes to produce catabolic proteinases that degrade the cartilage extracellular matrix. The pericellular matrix immediately adjacent to chondrocytes is thought to play a central role in transducing mechanical stimuli to biochemical signals within the cells.[1] For example, loading of cartilage causes release of fibroblast growth factor 2 (FGF2) from the pericellular matrix, and activates downstream extracellular signal–regulated kinase (ERK) signalling pathways in chondrocytes.[2, 3] FGF2 is localized in the pericellular matrix through its interaction with the heparan sulfate (HS) chains of perlecan,[2] the major HS proteoglycan in cartilage. Pericellular matrix and cell surface HS also binds to a large number of other bioactive proteins, including growth factors [eg, connective tissue growth factor (CTGF) and transforming growth factor β (TGFβ)], morphogens [eg, bone morphogenetic protein (BMP)-4 and BMP-7], proteinases [eg, matrix metalloproteinase 13 (MMP-13), adamalysin with thrombospondin motifs 4 (ADAMTS-4), and ADAMTS-5], and proteinase inhibitors (eg, tissue inhibitor of metalloproteinases, TIMP-3), and regulates their retention, localization, and biological activity.[4, 5] HS is thus a critical regulator of chondrocyte homeostasis and cartilage health. Previous studies have shown increased expression of some of the HS core proteins in OA, including perlecan,[6-9] syndecan 1[9-11], and syndecan 4,[11-13] but nothing is yet known about how the structure of HS itself or its interactions with ligands changes in OA.

HS interacts with proteins through electrostatic interactions between its negatively charged sulfate groups and positively charged lysine and arginine residues on the protein ligand. The number and arrangement of sulfate groups along the HS glycosaminoglycan chain determines the affinity of HS for its protein ligands and its ability to modulate their biological activity.[14-16] This sulfation pattern is

generated by the template-independent action of a series of sulfotransferases during HS synthesis in the Golgi apparatus.[17] The EXT family of glycosyltransferases initiate HS synthesis by adding sequential glucuronic acid (GlcA) and N-acetyl glucosamine (GlcNAc) residues to a linker tetrasaccharide attached to the core protein. GlcA can subsequently be epimerized to iduronic acid (IdoA) by glucuronyl C5-epimerase (GLCE). The growing HS chain can then be N-sulfated on GlcNAc residues [by the N-deacetylase/N-sulfotransferases (NDSTs)], and/or O-sulfated on GlcNAc [by the 6-O-sulfotransferases (HS6STs) and 3-O-sulfotransferases (HS3ST)] and GlcA/IdoA [by the 2-O-sulfotransferase (HS2ST1)].[17] HS can also be edited in the extracellular environment by SULF1 and SULF2 that remove 6-O-sulfate groups, or degraded by the heparanases HSPE1 and HSPE2. These reactions do not always occur to completion, generating a highly variable sulfation pattern that gives HS a structural complexity several orders of magnitude larger than the proteome. Temporal and spatial changes in HS sulfation occur during development[18-21] and in diseases such as Alzheimer disease[22, 23], cancer,[24] diabetes,[25] and fibrosis,[26] and are thought to enable HS to coordinately regulate the retention and activity of multiple bioactive ligands, and thus to powerfully regulate tissue homeostasis.

Here, we isolated RNA from knee cartilage of normal and osteoarthritic donors, and profiled expression of the 13 core proteins and 25 biosynthesis and modifying enzymes that govern HS structure and sulfation. Notably, disaccharide composition was examined by isolating HS from normal and OA cartilage. HS enzyme expression and glycan structure were found to be markedly dysregulated in OA cartilage, and increased 6-O-sulfation of HS was identified as the primary structural change associated with impaired cartilage homeostasis.

Materials and Methods

Human cartilage samples

Human articular cartilage was obtained in full compliance with national and institutional ethical requirements, the United Kingdom Human Tissue Act, and the Declaration of Helsinki.

Normal human knee cartilage specimens used for RNA and glycosaminoglycan analyses were obtained from Articular Engineering LLC (Northbrook, IL) from donors (six females of 44 to 68 years of age, six males of 32 to 75 years of age) with clinically healthy, normal cartilage and no history of OA, following informed donor consent and approval by local ethics committees and the University of Oxford Research Ethics Committee (R45926/RE001). Cartilage was aseptically harvested within 48 hours of death, flash frozen in liquid nitrogen, stored at -80 ^{o}C, and shipped in dry ice.

Normal human knee cartilage specimens used for immunohistochemistry were obtained from Stanmore Biobank (Royal National Orthopaedic Hospital, Stanmore) from donors undergoing amputation for low limb malignancies with no involvement of the cartilage, following informed donor consent and approval by the Royal Veterinary College Ethics and Welfare Committee (Institutional approval Unique Reference Number 2012 0048H). Cartilage was aseptically harvested from all surfaces of the joint within four hours of surgery and processed for downstream analyses.

Human OA cartilage samples used for immunohistochemistry, RNA, and glycosaminoglycan analyses were obtained from the Oxford Musculoskeletal Biobank from donors (six females of 58 to 83 years of age, six males of 52 to 84 years of age) undergoing total knee replacement surgery for advanced OA, following informed consent and approval by the Oxford Research Ethics Committee C (09/H0606/11). Cartilage was aseptically harvested from all surfaces of the joint within four hours of surgery and processed for downstream analyses.

RNA isolation

Cartilage (300 mg) from 12 normal and 12 OA donors was ground under liquid nitrogen with a pestle and mortar. The ground cartilage powder was added to 1.5 mL of RLT lysis buffer supplemented with 10 µL/mL β-mercaptoethanol (QIAGEN, UK), digested with proteinase K (6-10 mAU/100 mg of cartilage, 10 min at 55 $^{\circ}$C, QIAGEN, UK) and transferred to an RNeasy micro column (QIAGEN, UK). RNA was extracted according to the manufacturers' protocol with an intermediate DNA digestion step. The eluted RNA was quantified on a Nanodrop spectrophotometer and examined on a

Bioanalyser (Agilent, UK). RNA from healthy and OA cartilage had comparable RINs (6-7.7) and RNA yields.

Reverse transcription and quantitative PCR

Total RNA (250 ng) was reverse transcribed to cDNA using a reverse transcription kit (ThermoFisher) and cDNA amplified on a Taqman low density array (Table 1). Fold changes against the control samples were calculated using the ΔΔCt method. For calculating the ΔCt, the average of the three normalizing genes (*18S, RLPL0,* and *GAPDH*) was used.

Extraction of HSPGs and disaccharide analysis

Approximately 300 mg of frozen cartilage explants were ground in a pestle and mortar under liquid nitrogen and the powder was placed in 1 mL of Trizol (ThermoFisher Scientific, UK). After phase separation with the addition of chloroform, the aqueous phase was added to equilibrated DEAE-Sephacel beads, washed with PBS and 0.25 M NaCl before elution with 2 M NaCl. The eluate was desalted on PD10 columns and freeze dried. The samples were then treated with DNase (QIAGEN, UK) and RNase, prior to incubation with chondroitinase ABC (Sigma Aldrich, UK), neuraminidase, keratanase, and pronase. Following the digestions, the samples were once more purified on DEAE beads and freeze dried. The rest of the procedure was as described before.[27] Briefly, samples were sequentially digested with heparanase I, II, and III (IBEX Technologies, UK), purified on C18 and graphite spin columns (ThermoFisher Scientific, UK) and labelled with BIODIPY hydrazine (ThermoFisher Scientific, UK) as previously described.[28] Finally, samples underwent ethanol precipitation to remove any copurified impurities. Samples were then analyzed by SAX HPLC using a Propac PA-1 strong anion-exchange column (4.6x250nm; Dionex, UK). Samples were eluted with a linear gradient of 0 to -1 M sodium chloride and isocratic sodium hydroxide (150 mM) over 30 min at 1 mL/min on a Shimadzu HPLC system. An inline fluorimeter was used to detect eluted peaks (excitation λ = 488 nm, emission λ = 520 nm). Previously calculated correction factors were applied

to quantitate the observed disaccharides.[27]

Immunofluorescence staining analysis

Upon receipt, cartilage explants were embedded in OCT (Thermofisher Scientific, UK) and frozen in isopentane for storage at -80 °C until sectioning. Samples were mounted on a cryostat (CM1860UV, Leica, Milton Keynes, UK) and 5 μm sections were cut and mounted on Superfrost Plus microscope slides (ThermoFisher Scientific, UK) and stored at -80 °C. Frozen sections were air dried for one hour at room temperature and fixed with neutral buffered formalin for 5 minutes at room temperature prior to their incubation in ice cold acetone for 10 minutes at -20 °C, and incubated at 37 °C for 30 minutes with 0.1 U chondroitinase ABC (Sigma, C3667) in 1x chondroitinase buffer (40 mM Tris-acetate, pH 8). The digested sections were blocked in 1% goat serum and 5% BSA in PBS for one hour at room temperature. After 15 minutes permeabilization with 0.1% Triton X-100 in PBS, sections were washed in PBS and the primary antibodies were applied diluted in block buffer overnight at 4 °C, or isotype antibodies as negative controls. The following antibodies were used: rat anti-perlecan (HSPG2) (1:1000, Millipore, UK), rabbit anti-GLCE (1:20, HPA04821, Atlas Antibodies, Sweden), rabbit anti-EXTL2 (1:100, NBP2-16394, Novus, UK), mouse anti-NDST1 (3 μg/mL, ab55296, Abcam, UK), rabbit anti-GPC1 (1:250, HPA303571, Sigma, UK) and rabbit anti-HS6ST1 (1:250, ab106195, Abcam, UK). After washing in PBS at room temperature, the appropriate secondary antibodies were added; either in combination, or in unison, goat anti-rat Alexa Fluor 488 (1:1000, Thermo Fisher Scientific, UK), goat anti-rabbit Alexa Fluor 568 (1:500, Thermo Fisher Scientific, UK), or goat anti-mouse Alexa Fluor 568 (1:500, Thermo Fisher Scientific, UK) in block buffer. The secondary antibodies were washed off with PBS after three hours at room temperature. Nuclei were stained with DAPI (1:200 in PBS, Thermo Fisher Scientific, UK) for one hour before a final wash in PBS and mounting in Prolong Diamond antifade (Thermo Fisher Scientific UK).

Sections were viewed under an Olympus BX51 fluorescent microscope (Olympus, UK). For each protein the optimal duration of exposure was determined as that giving a signal in positively stained sections and no detectable staining in negatively stained sections, and avoiding overexposure and

signal saturation. The exposures used were: HSPG2 200-250 ms, EXTL2 125 ms, GLCE 200 ms, GPC1 125 ms, NDST1 280-300 ms, and HS6ST1 275-300ms. Images were obtained from at least six random regions of the cartilage under a 40x lens and then analyzed on ImageJ as described previously.[29, 30] For representative images, the intensity of the red and green signal was adjusted for illustrative purposes. For quantification, raw unaltered images were analyzed.

Analysis of ERK phosphorylation in chondrocytes

Primary OA chondrocytes were isolated from freshly harvested human OA cartilage by chopping the tissue finely and incubating in DMEM with 10% fetal calf serum (Gibco/ThermoFisher Scientific, UK) and 1.5 mg/mL type II collagenase (Roche, Switzerland) (18 hours, 37 °C, with shaking at 180 rpm). The suspension was passed through a cell strainer, pelleted, and washed twice with medium. Isolated chondrocytes were cultured for seven days until confluent[31] and stored at -80 °C until required. For small interfering RNA (siRNA) transfection, chondrocytes ($3x10^5$/well) were transfected with 20 nM of either Silencer Select Negative control #1 or Silencer Select *HS6ST1* siRNA (s17978, Ambion/ThermoFisher Scientific, UK) using Lipofectamine 2000 (Gibco/ThermoFisher Scientific, UK) in serum free Opti-MEM I (ThermoFisher Scientific).[31] After four hours, the medium was replaced with DMEM containing 10% FCS and cell cultured for a further 72 hours.

To analyze ERK phosphorylation, siRNA-treated chondrocytes were cultured in serum-free DMEM for 24 hours, and treated with PBS recombinant human FGF2 (R&D Systems, USA) (20 ng/ mL, 10 min). Cells were then washed twice with ice-cold PBS and lyzed on ice in 150 µL RIPA buffer containing protease inhibitors (SIGMAFAST, Sigma-Aldrich, UK) and phosphatase inhibitors (20mM NaF, 100 mM Na_3VO_4, 100 mM beta-glycerophosphate, 100 mM sodium pyrophosphate). Lysates were centrifuged (5000 rpm, 3 min) and 20 µg of protein analyzed by immunoblotting using antibodies against phosphoERK1/2 (1:2500, E7028, Sigma-Aldrich, UK) and total ERK (1:5000, 4695S, Cell Signalling Technology, UK) in block buffer (5% milk/PBST). After 3x 5 min washes with PBST, the membranes were incubated with an AP-conjugated anti-rabbit secondary antibody

(1:2000, Promega, UK) and developed using Western Blue stabilized substrate (Promega, UK). Immunoblots were analyzed by densitometry using Phoretix 1D software (TotalLab, Newcastle-upon-Tyne, UK) and the levels of phospho-ERK normalized to total ERK for each treatment, and expressed relative to the corresponding untreated sample (defined as 1).

Efficacy of siRNA silencing was confirmed by isolating RNA from RIPA lysates (20 to 50 μL, diluted to 350 μL with RLT buffer containing 1% v/v β-mercaptoethanol) using RNeasy micro kits according to the manufacturer's protocol (QIAGEN, Germany). Isolated RNA was reverse transcribed and expression of *18S*, *GAPDH*, and *HS6ST1* quantified as described above.

Statistical analysis

All statistical tests, except correlations and linear regression models, were performed in Graphpad Prism version 7.0d. All other statistical tests were performed in R. All significant changes are annotated in the figures.

Power calculations were based on pilot data from four samples per group. According to the pilot experiments, the sample size required for a two-tailed t-test was calculated with an effect size of 1.5 (difference between means of 0.6 and standard deviation of 0.4) and type I error rate α at 5%, to be 12 samples per group. Therefore the groups were extended to the appropriate sizes.

Prior to performing any parametric test, groups were tested for normality using the D'Agostino and Pearson omnibus test.[32]

Two-way ANOVA was performed and the forest plots (Figure 1) examined to evaluate whether there was significant variation in the age or sex of the donors.

All tests on the PCR results were performed on the ΔΔCt values as they were normally distributed. Multiple two-tailed t-tests were performed, comparing the expression of each gene between the two groups. The derived *P*-values were corrected for multiplicity using the two-stage step-up method of Benjamini, Krieger and Yekutieli (BKY), with a false discovery rate cut-off at 5%.[33]

For HS disaccharide composition, site of sulfation and extent of sulfation, two-way ANOVA was performed, with a BKY multiplicity correction.

Hierarchical clustering was performed in R (https://www.r-project.org) using the package gplots ß and RColorBrewer. Canberra distance was employed as the clustering metric.

For analysis of immunofluorescence images, the background-corrected integrated intensity values per cell were aggregated for the normal and OA groups (n = 3 to 6 per group), and the cumulative distributions of signal were analyzed using the Kolmogorov-Smirnov test, since the values were not normally distributed.

Results

Expression of HS proteoglycan core proteins is disrupted in OA cartilage

RNA was isolated from normal and osteoarthritic tibial knee cartilage (n = 12 per group), and examined expression of 13 genes encoding HS proteoglycan core proteins. Genes with a significant change in expression are shown in Figure 1.

Expression of agrin (*AGRN*) and perlecan (*HSPG2*) was significantly increased in OA samples (multiple *t*-tests, BKY corrected q>0.05), whereas expression of betaglycan (TGF β receptor III, *TGFBR3*) was reduced.

Among the syndecan family, syndecan 2 (*SDC2*) was not differentially regulated between the groups, whereas expression of syndecan 4 (*SDC4*) was reduced in OA, and expression of syndecan 1 (*SDC1*) and syndecan 3 (*SDC3*) was increased. *SDC1* was the most strongly regulated of the HS core proteins, with mean expression increasing 17-fold in OA.

Glypican core proteins showed fewer changes in expression in OA cartilage, with only glypican 1 (*GPC1*) showing significantly higher expression in OA samples. Expression of glypican 4 (*GPC4*), glypican 5 (*GPC5*), and glypican 6 (*GPC6*) was not significantly regulated, and glypican 2 (*GPC2*) and glypican 3 (*GPC3*) were minimally expressed in both normal and OA cartilage.

Expression of HS biosynthesis and modifying enzymes was also disrupted in OA cartilage

Using the same samples, expression of 25 genes encoding HS biosynthesis and modifying enzymes was analyzed (Figure 1), and 10 of these were found to be expressed at higher levels in OA cartilage.

Expression of *EXT1* and *EXT2*, which extend the growing HS chain, was increased in OA, as was expression of the related *EXTL1* and *EXTL2* genes. *EXTL1* was the most strongly regulated of all the genes examined, showing a 24-fold increase in expression in OA. Expression of *EXLT3* was not significantly regulated. Mean expression of epimerase (*GLCE*), which epimerizes glucuronic acid (GluA) to iduronic acid (IdoA), was increased 2-fold in OA cartilage.

Mean expression of the N-sulfotransferase *NDST1* was 3-fold higher in OA cartilage. *NDST2* was expressed at similar levels in both sample groups, and *NDST3* and *NDST4* were not appreciably expressed in either normal or OA cartilage.

Expression of the 2-O-sulfotransferase *HS2ST1* was not significantly altered in OA samples. Of the seven isoforms of 3-O-sulfotransferase, only *HS3ST1* showed increased expression in OA cartilage, with expression of *HS3ST3A1* and *HS3ST3B1* not differentially regulated and four of the isoforms (*HS3ST2*, *HS3ST3*, *HS3ST5*, *HS3ST6*) not detectably expressed in cartilage. Among the three 6-O-sulfotransferases isoforms, expression of *HS6ST1* was increased in OA cartilage, whereas *HS6ST3* expression was similar in both sample groups and *HS6ST2* was expressed at low levels.

Expression of both *SULF1* and *SULF2* was increased in OA cartilage, with *HSPE* and *HSPE2* not differentially expressed.

Cluster analysis of the samples, based on the levels of the significantly regulated genes, separated the samples into two clusters (Figure 2), with the first cluster containing all the OA samples and one of the normal samples, and the second cluster containing the remaining normal samples. This indicates that levels of expression of the 17 significantly regulated genes are largely able to discriminate normal and osteoarthritic cartilage.

Selected immunohistochemical analyses validate observed changes in expression

To establish whether the observed gene regulation resulted in corresponding changes in protein expression, six proteins (HSPG2, EXTL2, GLCE, NDST1, HS6ST1 and GPC1) were selected to

analyze by semi-quantitative immunofluorescence staining on frozen sections of normal and OA cartilage. HSPG2 was selected as a marker of pericellular matrix localization, and the other five proteins according to functional antibody availability and to have at least one from each category of HS core proteins and biosynthetic enzymes. The intensity of staining did not vary with cartilage depth for any of the antibodies examined.

As expected, HSPG2 exhibited a predominantly pericellular localization,[34] with approximately 50% increased expression per cell in the four OA samples examined compared to the six normal cartilage samples.

EXTL2 had a predominantly perinuclear localization in both normal and OA cartilage (Figure 3A). In OA cartilage, expression of EXTL2 was increased 1.6-fold, with a decrease in the number of cells not expressing EXTL2 and a shift towards more cells expressing moderate amounts of the protein (Figure 3B).

GLCE was similarly localized in the perinuclear region of cells (Figure 3C), with 2.4-fold higher expression in OA and a shift towards more cells expressing modest amount of the enzyme (Figure 3D).

HS6ST1 intensity levels were approximately three times higher in OA (Figure 4B). The protein appeared to be expressed at low levels around the nucleus in normal cartilage and to show some pericellular staining in the OA samples (Figure 4A).

NDST1 was localized in the perinuclear region in normal cells, with more expression towards the periphery of the cell and overlapping with HSPG2 in the OA samples (Figure 4C). Intensity levels were approximately 3.6-fold higher in the OA samples (Figure 4D).

Staining for GPC1 was predominantly intracellular (Figure 5A), with 5.5-fold higher intensity in OA samples (Figure 5B).

Increased 6-O-sulfation of HS in OA cartilage

The amount and disaccharide composition of HS isolated from normal and OA cartilage was analyzed (n = 8 per group, Figure 6A).

There was no significant difference in the total amount of HS in the normal and OA cartilage samples (5.7 ± 2.3 μg/100 mg in the normal samples, 3.0 ± μg/100 mg of tissue in OA, P >0.05 by *t*-test, Figure 6B), or in the ratio of sulfated to total HS disaccharides (36.5 % in normal cartilage, 53% in OA cartilage, Mann Whitney test, $P > 0.05$, Figure 6C).

Normal and OA cartilage did not differ significantly in the abundance of any single HS disaccharide (Figure 6D), or in the percentages of non-, mono-, di-, or triple-sulfated disaccharides (not shown). However, the percentage of 6-O-sulfated disaccharides was increased in OA cartilage (19.8% vs 12.1%, Mann Whitney test, $P = 0.0379$, Figure 6E).

6-O-sulfation of HS correlates with expression of GLCE, HS6ST1, EXTL2, and HS3ST3A1

It was examined whether expression of any of HS biosynthesis genes correlated with the HS disaccharide compositions quantified.

The percentage of 6-O-sulfated disaccharides correlated with expression of *HS6ST1* (r = 0.74, $P = 0.0016$, Figure 6F), *GLCE* (r = 0.775, $P = 0.0007$, Figure 6G), *EXTL2* (r = 0.57, $P = 0.026$), and *HS3ST3A1* (r = 0.575, $P = 0.025$). The relationship between 6-O-sulfation and *HS6ST1* expression was linear, with a 4% increase in abundance of 6-O-sulfated disaccharides for every doubling in the amount of *HS6ST1* (adjusted $R^2 = 0.525$, $P = 0.0014$). This relationship was independent of age, OA, and sex. The relationship between 6-O-sulfation and *GLCE* expression was linear, with a doubling in expression of GLCE increasing the percentage of 6-O-sulfation by about 4%. This relationship was dependent on age and sex, such that for every year increase in age there was a 0.17% increase in percent 6-O-sulfation, and that females had about 4% more 6-O-sulfation for the same amount of GLCE (adjusted $R^2 = 0.42$, $P = 0.028$).

The percentage of 2-O-sulfated disaccharides correlated with expression of *HS3ST3A1* (r = 0.796, $P = 0.0004$) and *HS6ST1* (r = 0.57, $P = 0.026$). The relationship between 2-O-sulfation and *HS3ST3A1* expression was linear, with a doubling in the levels of *HS3ST3A1* increasing the percentage of 2-O-sulfated disaccharides by 4%. This association was OA- and sex-dependent, such that females with OA had a 0.62% increase in 2-O-sulfation for the same level of

*HS3ST3A1*expression (adj $R^2 = 0.67$, $P = 0.0036$).

Correlations were also examined between expression of HS biosynthesis genes and the relative abundance of individual disaccharide residues. This showed that *HS3ST3A1* expression correlated with the percentage of UA(2S)-GlcNAc (r = 0.772, $P < 0.05$), UA(2S)-GlcNS (r = 0.538, $P < 0.05$), and UA-GlcNS(6S) (r = 0.521, $P < 0.05$), whereas *HS6ST1* expression correlated with the percentage of UA(2S)-GlcNAc (r = 0.53, $P < 0.05$), UA-GlcNAc(6S) (r = 0.58, $P < 0.05$), and UA-GlcNAc (r = -0.686, $P = 0.005$).

Finally, *HS3ST2* expression was found to be linearly associated with age, independent of OA and sex, with expression of *HS3ST2* increasing by 6% to 21% every year (adj R^2 =0.341, $P = 0.035$).

siRNA silencing of HS6ST1 inhibits FGF2 signalling

To investigate whether changes in HS6ST1 expression and 6-O-sulfation have the capacity to alter signalling in OA chondrocytes, chondrocytes were isolated from knee cartilage of five donors with late-stage OA, and FGF2-dependent ERK phosphorylation examined after siRNA knockdown of *HS6ST1*. siRNA treatment suppressed *HS6ST1* mRNA levels by >90% in all five donors (Figure 6H). Addition of 20 ng/mL FGF-2 stimulated rapid phosphorylation of ERK, and this was significantly reduced (by 40%) in *HS6ST1*-silenced cells (Figure 6I).

Discussion

HS proteoglycans control the retention, localization, and biological activity of over 400 bioactive molecules, including growth factors (eg, FGF2, TGFβ), morphogens (eg, BMP-4, BMP-7), proteinases (eg, MMP-13, ADAMTS-4, ADAMTS-5), and proteinase inhibitors (eg, TIMP-3).[4, 35-37] Many HS ligands have significant impacts on cartilage homeostasis, making HS a critical regulator of joint health. Despite this important role, nothing was previously known about how the structure and sulfation pattern of HS may change during the development of osteoarthritis. This study shows that the expression of HS biosynthesis and modifying enzymes and the resulting HS disaccharide

composition differs significantly in normal and osteoarthritic human knee cartilage.

Expression of the HS polymerases *EXT1* and *EXT2*, as well as *EXTL1* and *EXTL2*, was significantly increased in OA cartilage. The roles of these enzymes in homeostasis of adult cartilage has not been explored, but EXT1 and EXT2 are known to be important in musculoskeletal development. EXT1 regulates Ihh signalling during endochondral ossification,[38] and mutations in both EXT1 and EXT2 are associated with development of hereditary multiple exostoses, an inherited pediatric disorder characterized by osteochondroma formation.[39] Aberrant activation of chondrocyte hypertrophy has been implicated in development of OA,[40] and may underlie the elevated expression of *EXT1* and *EXT2* observed. The role of the related *EXTL* genes in HS synthesis are less well understood, but they are thought to regulate early stages of HS chain elongation.[41] Mutations in EXTL3 have been shown to impair musculoskeletal development,[42] and although *EXTL3* expression was not regulated in OA, expression of both *EXTL1* and *EXTL2* was strongly up-regulated.

Once polymerized, the HS chain can be modified by epimerization of GlcA to IdoA by a glucuronyl epimerase (GLCE), or by addition of sulfate groups to specific positions in the disaccharide units, by multiple sulfotransferases. The expression of 11 human HS sulfotransferases was measured and it was found that the expression of *NDST1*, *HS3ST1,* and *HS6ST1* was elevated in OA cartilage. Most notably, a significant increase was observed in the level of 6-O-sulfated disaccharides in OA cartilage, which correlated strongly with expression of both *HS6ST1* and *GLCE*. Epimerization of GlcA to IdoA by GLCE is thought to favor subsequent 6-O-sulfation,[43] suggesting that these two enzymes drive the increase in 6-O-sulfation in OA cartilage. Previous studies have shown that levels of 6-O-sulfation are spatially and temporally regulated during development,[18, 19, 21] and in diseases such as fibrosis,[44, 45] Alzheimer disease,[22] and cancer.[46, 47] In the case of fibrosis, a doubling in 6-O-sulfation is thought to exacerbate disease by amplifying TGFβ[44] and FGF-2[45] signaling. We hypothesized that increased 6-O-sulfation in OA cartilage may similarly amplify downstream signalling pathways and alter tissue homeostasis. Consistent with this, using primary OA chondrocytes isolated from five different donors, it was found that siRNA silencing of *HS6ST1* suppressed ERK phosphorylation in response to FGF2. This is in line with previous studies showing that 6-O-sulfation of HS promotes FGF2 signalling,[48-51] and confirms that changes in 6-O-sulfation

can alter biologically relevant signalling pathways in cartilage. 6-O-sulfation is known to alter HS affinity for a range of ligands,[52] with varying effects on their downstream activity. For example, 6-O-sulfation promotes TGFβ[53, 54] signalling, and inhibits Wnt[55, 56] and BMP[57, 58] signalling. An unbiased approach such as phosphoproteomics will be required to identify pathways regulated by 6-O-sulfation in normal and OA cartilage.

The importance of 6-O-sulfation is underscored by the fact that it is the only HS modification that is regulated at both the 'on' and the 'off' level, being added during HS biosynthesis in the Golgi apparatus by HS6ST1, HS6ST2, and/or HS6ST3[43], and removed in the extracellular environment by the 6-O-endosulfatases SULF1 and/or SULF2.[59] This permits "remodelling" of HS sulfation that is apparently critical to regulation of its functions. Indeed, increased expression of SULF1 and SULF2 was observed in OA cartilage, in line with previous reports examining both human and murine OA cartilage.[7, 9, 11, 58, 60, 61] Despite this, net levels of 6-O-sulfation were increased in our OA cartilage samples. As noted in recent studies from HS in muscle,[27] this highlights the importance of analysing HS structure directly, and may indicate post-translational regulation of HS6ST and/or SULF activity, or differences in the catalytic efficiency, location, or stability of the enzymes. *Sulf1*$^{-/-}$ and *Sulf2*$^{-/-}$ mice developed accelerated OA and injection of recombinant SULF1 into the joint reduced cartilage damage,[62] indicating the enzymes play a chondroprotective role. Elevated 6-O-sulfation may contribute to or perpetuate cartilage damage, potentially through driving anabolic pathways or impairing catabolic repair mechanisms.

No increase was seen in N-sulfation in OA cartilage, despite increased expression of NDST1 at the mRNA and protein level. The abundance of 3-O-sulfated disaccharides was not quantified due to their relative scarcity, but expression of *HS3ST1* was elevated in OA samples. Further investigation may be warranted as knowledge of the functional impact of 3-O-sulfation and the extent of the 3-O-proteome expands.[63, 64]

With regards to the HS core proteins the previously reported increase in expression of HSPG2[6-9], glypican 1,[11] syndecan 1[9-11], and syndecan 3[65] was observed in OA cartilage, but not the previously observed increase in syndecan 4[9, 11-13] or decrease in agrin.[66] This may suggest species- or joint-specific variation in expression of these genes. Additionally, the expression of many HS-associated

genes was significantly altered by isolation and culture of chondrocytes (data not shown), suggesting that HS biosynthesis is dynamically regulated by the chondrocyte microenvironment and that expression may change during the course of OA development.

A significant reduction was observed in the expression of TGFBR3 in OA cartilage. This HS core protein, also known as beta-glycan, does not have the ability to signal directly, but promotes TGFβ signalling by recruiting the growth factor and presenting it to the type II TGFβ receptor. In chondrocytes, TGFBR3 was recently shown to promote activation of latent TGFβ in a CTGF- and HS-dependent manner.[67] Reduction in expression of TGFBR3 in OA is thus likely to impair the chondroprotective effects of TGFβ signalling.

Previous rodent microarray studies indicate that expression of some HS core proteins, biosynthesis, and modifying enzymes is regulated early in the course of OA development.[7, 8, 11, 68-72] For example, expression of *Ext1*,[11, 68] *Sdc1*, [11, 68, 69] *Gpc1*, [11, 69] and *Hspg2*[11, 68] is significantly increased within two to four weeks of surgical OA induction (Supplementary Table S1[70-72]), in line with our findings here. Data on early changes in expression of sulfotransferases are variable, and early changes in *Hs6st1* were not reported. This may suggest that expression of this gene is stimulated once cartilage damage starts to escalate, but may also reflect differences between rodent post-traumatic OA and more variable human disease.

Age is a primary risk factor for the development of OA, and it is important to understand the cellular mechanisms that increase risk with age if we are to develop effective therapies to treat the disease. Previous studies have shown that HS sulfation patterns change with age in various tissues, including the aorta,[73] myocardium,[74] muscle stem cell niche[27], and brain,[75, 76] with concomitant changes in growth factor signalling. Although this study was not powered to detect changes in HS disaccharide composition with age, the expression of *HS3ST2* in cartilage was found to increase with age, in contrast to what has previously been reported in skin.[77] However, this observation is based on a low number of individuals (n = 11) as some values were missing for *HS3ST2* expression. Further analysis of age-dependent changes in HS structure may identify changes that impair cartilage repair with age and so increase the risk of OA after injury.

Our analysis identified 6-O-sulfation as the primary HS motif that is altered in end-stage OA

cartilage, validating it as a new target for potential therapeutic interventions. To understand the impact this change has on cartilage repair and OA progression, it will be necessary to perform unbiased analyses of the 6-O-sulfate-binding proteome in normal and OA cartilage. Comparative mass spectrometry approaches have proved useful in examining the 3-O-sulfate-binding proteome in cultured cells,[64] and similar methods could be developed for cartilage analysis. Analysis of other joint tissues (eg, bone, synovium, meniscus) and earlier stages of OA progression can also be expected to shed further light on the role of HS in adult joint homeostasis.

References

1. Sanchez-Adams J, Leddy HA, McNulty AL, O'Conor CJ, Guilak F: The mechanobiology of articular cartilage: bearing the burden of osteoarthritis. Curr Rheumatol Rep 2014, 16:451.
2. Vincent TL, McLean CJ, Full LE, Peston D, Saklatvala J: FGF-2 is bound to perlecan in the pericellular matrix of articular cartilage, where it acts as a chondrocyte mechanotransducer. Osteoarthritis Cartil 2007, 15:752-63.
3. Vincent TL, Hermansson MA, Hansen UN, Amis AA, Saklatvala J: Basic fibroblast growth factor mediates transduction of mechanical signals when articular cartilage is loaded. Arthritis Rheum 2004, 50:526-33.
4. Ori A, Wilkinson MC, Fernig DG: A systems biology approach for the investigation of the heparin/heparan sulfate interactome. J Biol Chem 2011, 286:19892-904.
5. Vincent TL: Targeting mechanotransduction pathways in osteoarthritis: a focus on the pericellular matrix. Curr Opin Pharmacol 2013, 13:449-54.
6. Tesche F, Miosge N: Perlecan in late stages of osteoarthritis of the human knee joint. . Osteoarthr Cartil 2004, 12:852-62.
7. Karlsson C, Dehne T, Lindahl A, Brittberg M, Pruss A, Sittinger M, Ringe J: Genome-wide expression profiling reveals new candidate genes associated with osteoarthritis. Osteoarthritis Cartilage 2010, 18:581-92.
8. Sato T, Konomi K, Yamasaki S, Aratani S, Tsuchimochi K, Yokouchi M, Masuko-Hongo K, Yagishita N, Nakamura H, Komiya S, Beppu M, Aoki H, Nishioka K, Nakajima T: Comparative analysis of gene expression profiles in intact and damaged regions of human osteoarthritic cartilage. Arthritis Rheum 2006, 54:808-17.
9. Loeser RF, Olex AL, McNulty MA, Carlson CS, Callahan MF, Ferguson CM, Chou J, Leng X, Fetrow JS: Microarray analysis reveals age-related differences in gene expression during the development of osteoarthritis in mice. Arthritis Rheum 2012, 64:705-17.

10. Salminen-Mankonen H, Säämänen a-M, Jalkanen M, Vuorio E, Pirilä L: Syndecan-1 expression is upregulated in degenerating articular cartilage in a transgenic mouse model for osteoarthritis. Scand J Rheumatol 2005, 34:469-74.
11. Gardiner MD, Vincent TL, Driscoll C, Burleigh A, Bou-Gharios G, Saklatvala J, Nagase H, Chanalaris A: Transcriptional analysis of micro-dissected articular cartilage in post-traumatic murine osteoarthritis. Osteoarthritis Cartil 2015, 23:616-28.
12. Barre P, Redinif F, Boumedienef K, Vielpeau C, Pujolf J: Semiquantitative reverse transcription-polymerase chain reaction analysis of syndecan-1 and -4 messages in cartilage and cultured chondrocytes from osteoarthritic joints. . Osteoarthr Cartil 2000, 8:34-43
13. Echtermeyer F, Bertrand J, Dreier R, Meinecke I, Neugebauer K, Fuerst M, Lee YJ, Song YW, Herzog C, Theilmeier G, Pap T: Syndecan-4 regulates ADAMTS-5 activation and cartilage breakdown in osteoarthritis. Nature Medicine 2009, 15:1072-6.
14. Guimond SE, Turnbull JE: Fibroblast growth factor receptor signalling is dictated by specific heparan sulfhate saccharides. Curr Biol 1999, 9:1343-6.
15. Shipp EL, Hsieh-Wilson LC: Profiling the sulfation specificities of glycosaminoglycan interactions with growth factors and chemotactic proteins using microarrays. Chem Biol 2007, 14:195-208.
16. Ashikari-Hada S, Habuchi H, Kariya Y, Itoh N, Reddi AH, Kimata K: Characterization of growth factor-binding structures in heparin/heparan sulfate using an octasaccharide library. J Biol Chem 2004, 279:12346-54.
17. Kreuger J, Kjellén L: Heparan sulfate biosynthesis: regulation and variability. J Histochem Cytochem 2012, 60:898-907.
18. Brickman Y, Nurcombe V, Gallagher J, Ford M, Turnbull J: Structural modification of FGF-binding HS at a determinative stage of neuroepithelial development. J Biol Chem 1998, 273:4350-9.
19. Kalus I, Rohn S, Puvirajesinghe TM, Guimond SE, Eyckerman-Kölln PJ, Ten Dam G, van Kuppevelt TH, Turnbull JE, Dierks T: Sulf1 and Sulf2 differentially modulate heparan sulfate

proteoglycan sulfation during postnatal cerebellum development: evidence for neuroprotective and neurite outgrowth promoting functions. PLoS One 2015, 10:e0139853.

20. Thompson SM, Fernig DG, Jesudason EC, Losty PD, van de Westerlo EM, van Kuppevelt TH, Turnbull JE: Heparan sulfate phage display antibodies identify distinct epitopes with complex binding characteristics: insights into protein binding specificities. J Biol Chem 2009, 284:35621-31.
21. Buresh-Stiemke RA, Malinowski RL, Keil KP, Vezina CM, Oosterhof A, Van Kuppevelt TH, Marker PC: Distinct expression patterns of Sulf1 and Hs6st1 spatially regulate heparan sulfate sulfation during prostate development. Dev Dyn 2012, 241:2005-13.
22. Hosono-Fukao T, Ohtake-Niimi S, Hoshino H, Britschgi M, Akatsu H, Hossain M, Nishitsuji K, van Kuppevelt T, Kimata K, Michikawa M, Wyss-Coray T, Uchimura K: Heparan sulfate subdomains that are degraded by Sulf accumulate in cerebral amyloid ß plaques of Alzheimer's disease: evidence from mouse models and patients. Am J Pathol 2012, 180:2056-67.
23. Sepulveda-Diaz JE, Alavi Naini SM, Huynh MB, Ouidja MO, Yanicostas C, Chantepie S, Villares J, Lamari F, Jospin E, van Kuppevelt TH, Mensah-Nyagan AG, Raisman-Vozari R, Soussi-Yanicostas N, Papy-Garcia D: HS3ST2 expression is critical for the abnormal phosphorylation of tau in Alzheimer's disease-related tau pathology. Brain 2015, 138:1339-54.
24. Bernsen M, Smetsers T, van de Westerlo E, Ruiter D, Håkansson L, Gustafsson B, van Kuppevelt T, Krysander L, Rettrup B, Håkansson A: Heparan sulphate epitope-expression is associated with the inflammatory response in metastatic malignant melanoma. Cancer Immunol Immunother 2003, 52:780-3.
25. Wijnhoven T, Lensen J, Rops A, van der Vlag J, Kolset S, Bangstad H, Pfeffer P, van den Hoven M, Berden J, van den Heuvel L, van Kuppevelt T: Aberrant heparan sulfate profile in the human diabetic kidney offers new clues for therapeutic glycomimetics. Am J Kidney Dis 2006, 48:250-61.
26. Westergren-Thorsson G, Hedström U, Nybom A, Tykesson E, Åhrman E, Hornfelt M, Maccarana M, van Kuppevelt TH, Dellgren G, Wildt M, Zhou XH, Eriksson L, Bjermer L, Hallgren O:

Increased deposition of glycosaminoglycans and altered structure of heparan sulfate in idiopathic pulmonary fibrosis. Int J Biochem Cell Biol 2017, 83:27-38.

27. Ghadiali RS, Guimond SE, Turnbull JE, Pisconti A: Dynamic changes in heparan sulfate during muscle differentiation and ageing regulate myoblast cell fate and FGF2 signalling. Matrix Biol 2017, 59:54-68.
28. Skidmore MA, Guimond SE, Dumax-Vorzet AF, Atrih A, Yates EA, Turnbull JE: High sensitivity separation and detection of heparan sulfate disaccharides. J Chromatogr A 2006, 1135:52-6.
29. Barbáchano A, Ordóñez-Morán P, García JM, Sánchez A, Pereira F, Larriba MJ, Martínez N, Hernández J, Landolfi S, Bonilla F, Pálmer HG, Rojas JM, Muñoz A: SPROUTY-2 and E-cadherin regulate reciprocally and dictate colon cancer cell tumourigenicity. Oncogene 2010, 29:4800-13.
30. Tenbaum S, Arqués O, Chicote I, Tenbaum S, Puig I, G. Palmer H: Standardized relative quantification of immunofluorescence tissue staining. Protocol Exchange 2012:doi:10.1038/protex.2012.008.
31. Ismail HM, Miotla-Zarebska J, Troeberg L, Tang X, Stott B, Yamamoto K, Nagase H, Fosang AJ, Vincent TL, Saklatvala J: JNK-2 controls aggrecan degradation in murine articular cartilage and the development of experimental osteoarthritis. Arthritis Rheumatol 2016, 68:1165-71.
32. Rani Das K, M Rahmatullah Imon AH, M Rahmatullah AH: A brief review of tests for normality. Am J Theor Appl Stat 2016, 5.
33. Benjamini Y, Krieger AM, Yekutieli D: Adaptive linear step-up procedures that control the false discovery rate. Biometrika 2006, 93:491-507.
34. Iozzo RV, Cohen IR, Grassel S, Murdoch AD: The biology of perlecan: the multifaceted heparan sulphate proteoglycan of basement membranes and pericellular matrices. Biochem J 1994, 302:625-39.
35. Sakamoto S, Goldhaber P, Glimcher M: Mouse bone collagenase. The effect of heparin on the amount of enzyme released in tissue culture and on the activity of the enzyme. Calcif Tissue Res 1973, 12:247-58.

36. Gao G, Plaas A, Thompson V, Jin S, Zuo F, Sandy J: ADAMTS4 (aggrecanase-1) activation on the cell surface involves C-terminal cleavage by glycosylphosphatidyl inositol-anchored membrane type 4-matrix metalloproteinase and binding of the activated proteinase to chondroitin sulfate and heparan sulfate on syndecan-1. J Biol Chem 2004, 279:10042-51.
37. Zeng W, Corcoran C, Collins-Racie L, Lavallie E, Morris E, Flannery C: Glycosaminoglycan-binding properties and aggrecanase activities of truncated ADAMTSs: comparative analyses with ADAMTS-5, -9, -16 and -18. Biochim Biophys Acta 2006, 1760:517-24.
38. Koziel L, Kunath M, Kelly O, Vortkamp A: Ext1-dependent heparan sulfate regulates the range of Ihh signaling during endochondral ossification. . Dev Cell 2004, 6:801-13.
39. Pacifici M: The pathogenic roles of heparan sulfate deficiency in hereditary multiple exostoses. Matrix Biol 2017, In press.
40. Sun MM, Beier F: Chondrocyte hypertrophy in skeletal development, growth, and disease. Birth Defects Res C Embryo Today 2014, 102:74-82.
41. Busse-Wicher M, Wicher KB, Kusche-Gullberg M: The exostosin family: proteins with many functions. Matrix Biol 2014, 35:25-33.
42. Notarangelo LD: Expanding the spectrum of skeletal dysplasia with immunodeficiency: a commentary on identification of biallelic EXTL3 mutations in a novel type of spondylo-epi-metaphyseal dysplasia. J Hum Genet 2017, 62:737-8.
43. Habuchi H, Tanaka M, Habuchi O, Yoshida K, Suzuki H, Ban K, K. K: The occurrence of three isoforms of heparan sulfate 6-O-sulfotransferase having different specificities for hexuronic acid adjacent to the targeted N-sulfoglucosamine. J Biol Chem 2000, 275:2859-6.
44. Lu J, Auduong L, White ES, Yue X: Up-regulation of heparan sulfate 6-O-sulfation in idiopathic pulmonary fibrosis. Am J Respir Cell Mol Biol 2014, 50:106-14.
45. Alhasan AA, Spielhofer J, Kusche-Gullberg M, Kirby JA, Ali S: Role of 6-O-sulfated heparan sulfate in chronic renal fibrosis. J Biol Chem 2014, 289:20295-306.
46. Ferreras C, Rushton G, Cole CL, Babur M, Telfer BA, van Kuppevelt TH, Gardiner JM, Williams KJ, Jayson GC, Avizienyte E: Endothelial heparan sulfate 6-O-sulfation levels regulate

angiogenic responses of endothelial cells to fibroblast growth factor 2 and vascular endothelial growth factor. J Biol Chem 2012, 287:36132-46.

47. Waaijer CJ, de Andrea CE, Hamilton A, van Oosterwijk JG, Stringer SE, Bovée JV: Cartilage tumour progression is characterized by an increased expression of heparan sulphate 6O-sulphation-modifying enzymes. Virchows Arch 2012, 461:475-81.
48. Pellegrini L, Burke DF, von Delft F, Mulloy B, Blundell TL: Crystal structure of fibroblast growth factor receptor ectodomain bound to ligand and heparin. Nature 2000, 407:1029-34.
49. Schlessinger J, Plotnikov AN, Ibrahimi OA, Eliseenkova AV, Yeh BK, Yayon A, Linhardt RJ, Mohammadi M: Crystal structure of a ternary FGF-FGFR-heparin complex reveals a dual role for heparin in FGFR binding and dimerization. Mol Cell 2000, 6:743-50.
50. Pye D, Vives R, Turnbull J, Hyde P, Gallagher J: Heparan sulfate oligosaccharides require 6-O-sulfation for promotion of basic fibroblast growth factor mitogenic activity. J Biol Chem 1998, 273:22936-42.
51. Jemth P, Kreuger J, Kusche-Gullberg M, Sturiale L, Giménez-Gallego G, Lindahl U: Biosynthetic oligosaccharide libraries for identification of protein-binding heparan sulfate motifs. Exploring the structural diversity by screening for fibroblast growth factor (FGF)1 and FGF2 binding. J Biol Chem 2002, 277:30567-73.
52. El Masri R, Seffouh A, Lortat-Jacob H, Vivès RR: The "in and out" of glucosamine 6-O-sulfation: the 6th sense of heparan sulfate. Glycoconj J 2017, 34:285-98.
53. Lyon M, Rushton G, Gallagher J: The interaction of the transforming growth factor-betas with heparin/heparan sulfate is isoform-specific. J Biol Chem 1997, 272:18000-6.
54. Yue X, Li X, Nguyen HT, Chin DR, Sullivan DE, Lasky JA: Transforming growth factor-beta1 induces heparan sulfate 6-O-endosulfatase 1 expression in vitro and in vivo. J Biol Chem 2008, 283:20397-407.
55. Ai X, Do AT, Lozynska O, Kusche-Gullberg M, Lindahl U, Emerson CPJ: QSulf1 remodels the 6-O sulfation states of cell surface heparan sulfate proteoglycans to promote Wnt signaling. J Cell Biol 2003, 162:341-51.

56. Dhoot G, Gustafsson M, Ai X, Sun W, Standiford D, Emerson CJ: Regulation of Wnt signaling and embryo patterning by an extracellular sulfatase. Science 2001, 293:1663-6.

57. Viviano BL, Paine-Saunders S, Gasiunas N, Gallagher J, Saunders S: Domain-specific modification of heparan sulfate by Qsulf1 modulates the binding of the bone morphogenetic protein antagonist Noggin. J Biol Chem 2004, 279:5604-11.

58. Otsuki S, Hanson SR, Miyaki S, Grogan SP, Kinoshita M, Asahara H, Wong C-H, Lotz MK: Extracellular sulfatases support cartilage homeostasis by regulating BMP and FGF signaling pathways. Proc Natl Acad Sci U S A 2010, 107:10202-7.

59. Morimoto-Tomita M, Uchimura K, Werb Z, Hemmerich S, Rosen S: Cloning and characterization of two extracellular heparin-degrading endosulfatases in mice and humans. J Biol Chem 2002, 277:49175-85.

60. Otsuki S, Taniguchi N, Grogan SP, D'Lima D, Kinoshita M, Lotz M: Expression of novel extracellular sulfatases Sulf-1 and Sulf-2 in normal and osteoarthritic articular cartilage. Arthritis Res Ther 2008, 10:R61.

61. Bateman JF, Rowley L, Belluoccio D, Chan B, Bell K, Fosang AJ, Little CB: Transcriptomics of wild-type mice and mice lacking ADAMTS-5 activity identifies genes involved in osteoarthritis initiation and cartilage destruction. Arthritis Rheum 2013, 65:1547-60.

62. Otsuki S, Murakami T, Okamoto Y, Hoshiyama Y, Oda S, Neo M: Suppression of cartilage degeneration by intra-articular injection of heparan sulfate 6-O endosulfatase in a mouse osteoarthritis model. Histol Histopathol 2017, 32:725-33.

63. Huang Y, Mao Y, Zong C, Lin C, Boons GJ, Zaia J: Discovery of a heparan sulfate 3-O-sulfation specific peeling reaction. Anal Chem 2015, 87:592-600.

64. Thacker BE, Seamen E, Lawrence R, Parker MW, Xu Y, Liu J, Vander Kooi CW, Esko JD: Expanding the 3-O-sulfate proteome - enhanced binding of neuropilin-1 to 3-O-sulfated heparan sulfate modulates its activity. ACS Chem Biol 2016, 11:971-80.

65. Pfander D, Swoboda B, Kirsch T: Expression of early and late differentiation markers (proliferating cell nuclear antigen, syndecan-3, annexin VI, and alkaline phosphatase) by human osteoarthritic chondrocytes. Am J Pathol 2001, 159:1777-83.

66. Eldridge S, Nalesso G, Ismail H, Vicente-Greco K, Kabouridis P, Ramachandran M, Niemeier A, Herz J, Pitzalis C, Perretti M, Dell'Accio F: Agrin mediates chondrocyte homeostasis and requires both LRP4 and α-dystroglycan to enhance cartilage formation in vitro and in vivo. Ann Rheym Dis 2016, 75:1228-35.

67. Tang X, Muhammad H, McClean C, Zarebska J, Flemming J, Didangelos A, Önnerfjord P, Leask A, Saklatvala J, Vincent TL: Connective tissus growth factor (CTGF) contributes to joint homeostasis and osteoarthritis severity by controlling the matrix sequestration and activation of latent TGFβ. Ann Rheum Dis 2018, 77:1372-80.

68. Loeser RF, Olex AL, McNulty MA, Carlson CS, Callahan M, Ferguson C, Fetrow JS: Disease progression and phasic changes in gene expression in a mouse model of osteoarthritis. PLoS One 2013, 8:e54633.

69. Appleton CTG, Pitelka V, Henry J, Beier F: Global analyses of gene expression in early experimental osteoarthritis. Arthritis Rheum 2007, 56:1854-68.

70. Geyer M, Grassel S, Straub RH, Schett G, Dinser R, Grifka J, Gay S, Neumann E, Muller-Ladner U: Differential transcriptome analysis of intraarticular lesional vs intact cartilage reveals new candidate genes in osteoarthritis pathophysiology. Osteoarthritis Cartilage 2009, 17:328-35.

71. Dunn SL, Soul J, Anand S, Schwartz JM, Boot-Handford RP, Hardingham TE: Gene expression changes in damaged osteoarthritic cartilage identify a signature of non-chondrogenic and mechanical responses. Osteoarthritis Cartilage 2016 24:1431-40.

72. Snelling S, Rout R, Davidson R, Clark I, Carr A, Hulley PA, Price AJ: A gene expression study of normal and damaged cartilage in anteromedial gonarthrosis, a phenotype of osteoarthritis. Osteoarthritis Cartilage 2014, 22:334-43.

73. Feyzi E, Saldeen T, Larsson E, Lindahl U, Salmivirta M: Age-dependent modulation of heparan sulfate structure and function. J Biol Chem 1998, 273:13395-8.

74. Huynh MB, Morin C, Carpentier G, Garcia-Filipe S, Talhas-Perret S, Barbier-Chassefière V, van Kuppevelt TH, Martelly I, Albanese P, Papy-Garcia D: Age-related changes in rat myocardium involve altered capacities of glycosaminoglycans to potentiate growth factor functions and heparan sulfate-altered sulfation. J Biol Chem 2012, 287:11363-73.

75. Huynh MB, Villares J, Díaz JE, Christiaans S, Carpentier G, Ouidja MO, Sissoeff L, Raisman-Vozari R, Papy-Garcia D: Glycosaminoglycans from aged human hippocampus have altered capacities to regulate trophic factors activities but not Aβ42 peptide toxicity. Neurobiol Aging 2012, 33:1005.e11-22.

76. Yamada T, Kerever A, Yoshimura Y, Suzuki Y, Nonaka R, Higashi K, Toida T, Mercier F, Arikawa-Hirasawa E: Heparan sulfate alterations in extracellular matrix structures and fibroblast growth factor-2 signaling impairment in the aged neurogenic niche. J Neurochem 2017, 142:534-44.

77. Glass D, Viñuela A, Davies MN, Ramasamy A, Parts L, Knowles D, Brown AA, Hedman ÅK, Small KS, Buil A, Grundberg E, Nica AC, Meglio P, Nestle FO, Ryten M, Durbin R, McCarthy MI, Deloukas P, Dermitzakis ET, Weale ME, Bataille V, Spector TD: Gene expression changes with age in skin, adipose tissue, blood and brain. Genome Biol 2013, 14:R75.

Figure legends

Figure 1. Changes in heparan sulfate (HS)-related gene expression in human osteoarthritis (OA) cartilage. Expression of HS-associated genes in normal and OA cartilage (n = 12 per group) was analyzed using Taqman low-density arrays. Fold changes in expression were determined by the ΔΔCt method against the average of the normal samples. **A:** Fold changes in expression of HS core protein genes. **B:** Fold changes in expression of HS chain elongation and sulfatase genes. **C:** Fold changes in expression of sulfotransferase genes. Error bars represent 95% of confidence intervals of the mean. **q <0.01, ***q < 0.001, ****q < 0.0001 by BKY corrected multiple *t*-test.

Figure 2. Expression of heparan sulfate (HS)-associated genes is altered in osteoarthritis (OA) cartilage. **A:** Forest plot showing there is no significant difference between the ages and sexes of normal (n = 12) and OA (n = 12) cartilage donors used for gene expression analysis. M, male; F, female. Bars show 95% confidence intervals of the mean, dotted line shows Y=0. **B:** Expression of HS-associated genes in normal and OA cartilage was analyzed using Taqman low-density arrays. Fold change in expression were determined by the ΔΔCt method against the average of the normal samples. The heatmap shows only those HS-associated genes whose expression was significantly different in the two groups (n = 12 for each group; BKY corrected multiple *t*-test; q-value < 0.05), with increased expression in OA shown in red, reduced expression shown in blue, and no change indicated in green. Cluster analysis based on the expression levels of significantly regulated genes separated the samples into two clusters, with the first cluster containing all of the OA samples and one of the normal samples, and the second cluster containing the remaining normal samples.

Figure 3. Expression of HSPG2, EXTL2, and GLCE is increased in human osteoarthritis (OA) cartilage. **A:** Representative images showing expression of HSPG2 and EXLT2 in human normal and OA cartilage. **B:** Expression of HSPG2 and EXLT2 was semi-quantitatively evaluated in three normal donors (N1, N2, and N3) and three OA donors (OA1, OA2, and OA3), with each dot representing integrated fluorescence intensity per single cell, calculated from at least six random fields of view on

three sections per donor. For each donor, the median fluorescence intensity with 95% confidence intervals of the mean are shown. **C:** Representative images showing expression of HSPG2 and GLCE in human normal and OA cartilage. **D:** Expression of HSPG2 and GLCE was semi-quantitatively evaluated in three normal donors (N4, N5 and N6) and three OA donors (OA1, OA2, and OA4) as described in **B**. $^{**}P < 0.01$, $^{***}P < 0.001$, $^{****}P < 0.0001$ by Kolmogorov-Smirnov test. Scale bar = 260 μm.

Figure 4. Expression of HSPG2, HS6ST1, and NDST1 is increased in human osteoarthritis (OA) cartilage. **A:** Representative images showing expression of HSPG2 and HS6ST1 in human normal and OA cartilage. **B:** Expression of HSPG2 and HS6ST1 was semi-quantitatively evaluated in three normal donors (N4, N5, and N6) and three OA donors (OA1, OA2, and OA4), with each dot representing integrated fluorescence intensity per cell, calculated from at least six random fields of view on three sections per donor. For each donor, the median fluorescence intensity with 95% confidence intervals of the mean are shown. **C:** Representative images showing expression of HSPG2 and NDST1 in human normal and OA cartilage. **D:** Expression of HSPG2 and NDST1 was semi-quantitatively evaluated in three normal donors (N1, N2, and N3) and three OA donors (OA1, OA2, and OA3) as described in **B**. $^{*}P < 0.05$, $^{****}P < 0.0001$ by Kolmogorov-Smirnov test. Scale bar = 260 μm.

Figure 5. Expression of HSPG2 and glypican 1 (GPC1) is increased in human osteoarthritis (OA) cartilage. **A:** Representative images showing expression of HSPG2 and GPC1 in human normal and OA cartilage. **B:** Expression of HSPG2 and GPC1 was semi-quantitatively evaluated in three normal donors (N1, N2, and N3) and three OA donors (OA1, OA2, and OA3), with each dot representing integrated fluorescence intensity per cell, calculated from at least six random fields of view on three sections per donor. For each donor, the median fluorescence intensity with 95% confidence intervals of the mean are shown. $^{**}P < 0.01$ by Kolmogorov-Smirnov test. Scale bar = 260 μm.

Figure 6. 6-O-sulfation is increases in osteoarthritis (OA) cartilage. Heparan sulfate (HS) was isolated from normal (n = 8) and OA (n = 8) cartilage and its composition analyzed by disaccharide analysis. **A:** Forest plot showing there is no significant difference between the ages and sexes of normal (n = 8) and OA (n = 8) cartilage donors used for HS analysis. M, male; F, female. Bars show 95% confidence intervals of the mean, dotted line shows Y=0. **B:** The total amount of HS in OA cartilage is not statistically different from that in normal cartilage. **C:** The ratio of sulfated to total HS is not statistically different between the two groups of samples. **D:** Abundance of individual disaccharide species is not significantly different in normal and OA cartilage. GlcNAc, N-acetyl glucosamine; GlcNS, *N*-sulfoglucosamine; UA, uronic acid; 2S, 2-O-sulfate; 6S, 6-O-sulfate. **E:** 6-O-sulfated HS disaccharides are more abundant in OA cartilage, whereas levels of N- and 2-O-sulfation are not significantly altered. **F:** The level of 6-O-sulfation in donor cartilage correlates with expression of HS6ST1 (n = 15, normal cartilage shown in black, OA cartilage in grey, males as squares, female samples as circles). **G:** The level of 6-O-sulfation in donor cartilage also correlates with expression of GLCE (n = 15, normal cartilage shown in black, OA cartilage in grey, males as squares, female samples as circles). **H**: Expression of *HS6ST1* in primary OA chondrocytes is silenced using siRNA (n = 5 donors). NT, transfected with non-targeting siRNA. **I**: Silencing of *HS6ST1* in primary OA chondrocytes reduces phosphorylation of ERK in response to FGF2 (20 ng/mL, 10 min) (n = 5 donors). **P* < 0.05, ***P* <0.01, ****P* < 0.001, multiple t-tests BKY corrected.

Table 1: Primer/probe sets used on custom-designed Taqman low density arrays.

Gene name	Primer/probe set
Chain elongation	
EXT1	Hs00609162_m1
EXT2	Hs00181158_m1
EXTL1	Hs00184929_m1
EXTL2	Hs01018237_m1
EXTL3	Hs00918601_m1
N-deacetylase/ N-sulfotransferases	
NDST1	Hs00925442_m1
NDST2	Hs00234335_m1
NDST3	Hs01128584_m1
NDST4	Hs00224024_m1
Glucuronyl C5-epimerase	
GLCE	Hs00392011_m1
2-O-sulfotransferase	
HS2ST1	Hs00202138_m1
3-O-sulfotransferases	
HS3ST1	Hs00245421_s1
HS3ST2	Hs00428644_m1
HS3ST3A1	Hs00925624_s1
HS3ST3B1	Hs00797512_s1
HS3ST4	Hs00901124_s1
HS3ST5	Hs00999394_m1
HS3ST6	Hs03007244_m1
6-O-sulfotransferases	
HS6ST1	Hs00757137_m1
HS6ST2	Hs02925656_m1
HS6ST3	Hs00542178_m1
Editing enzymes	
HSPE	Hs00935036_m1
HSPE2	Hs00222435_m1
SULF1	Hs00290918_m1
SULF2	Hs01016476_m1
Core proteins	
AGRN	Hs00394748_m1
GPC1	Hs00892476_m1
GPC2	Hs00415099_m1
GPC3	Hs01018936_m1
GPC4	Hs00155059_m1
GPC5	Hs00270114_m1
GPC6	Hs00170677_m1
HSPG2	Hs00194179_m1
SDC1	Hs00896423_m1
SDC2	Hs00299807_m1
SDC3	Hs01568665_m1
SDC4	Hs00161617_m1
TGFBR3	Hs01114253_m1
Normalizing genes	
18S	Hs99999901_s1
RPLP0	Hs99999902_m1
GAPDH	Hs99999905_m1

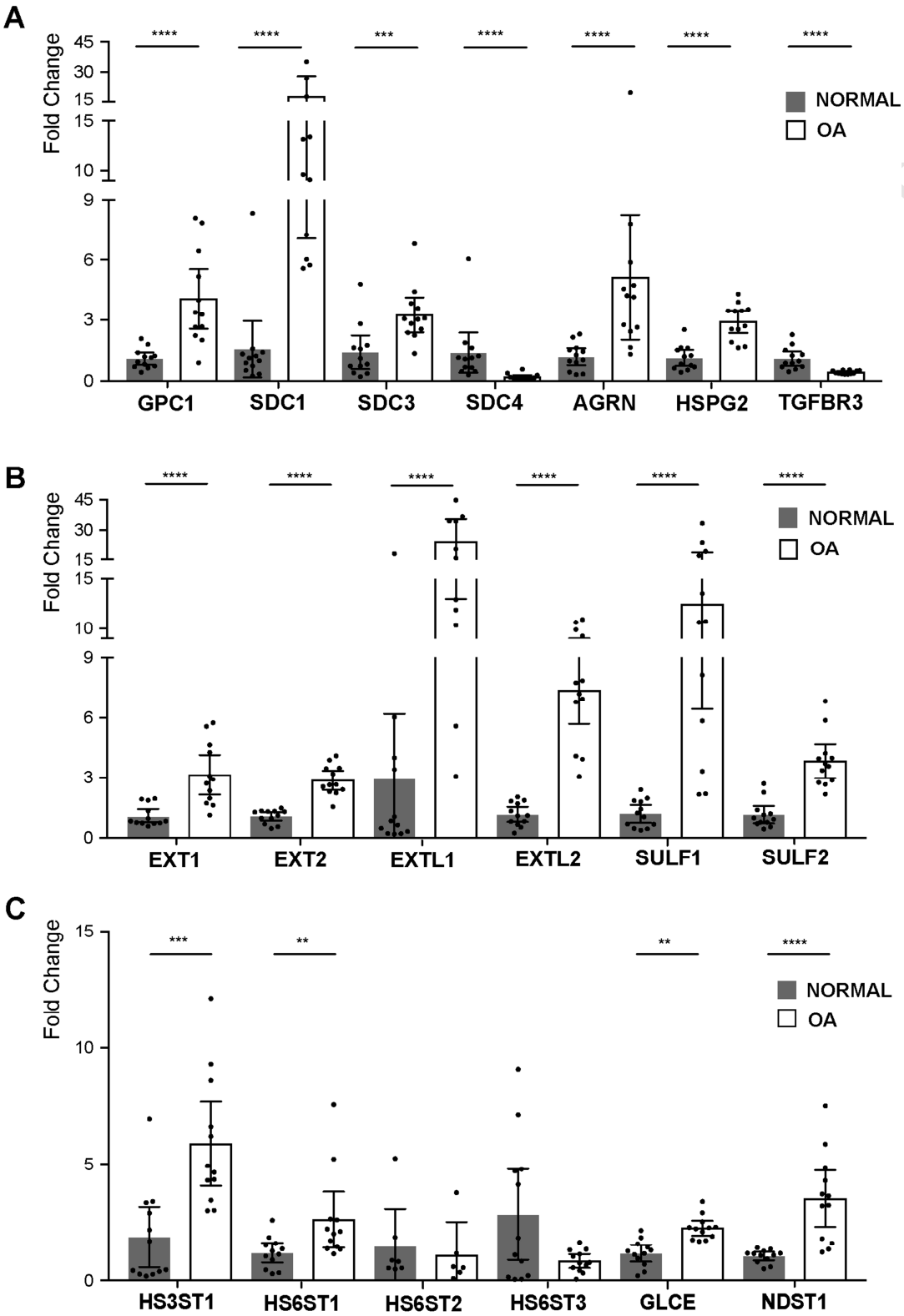
A
Fold Change
45
30
15
15
10
9
6
3
0
****
***
NORMAL
OA
GPC1
SDC1
SDC3
SDC4
AGRN
HSPG2
TGFBR3
B
EXT1
EXT2
EXTL1
EXTL2
SULF1
SULF2
C
**
HS3ST1
HS6ST1
HS6ST2
HS6ST3
GLCE
NDST1

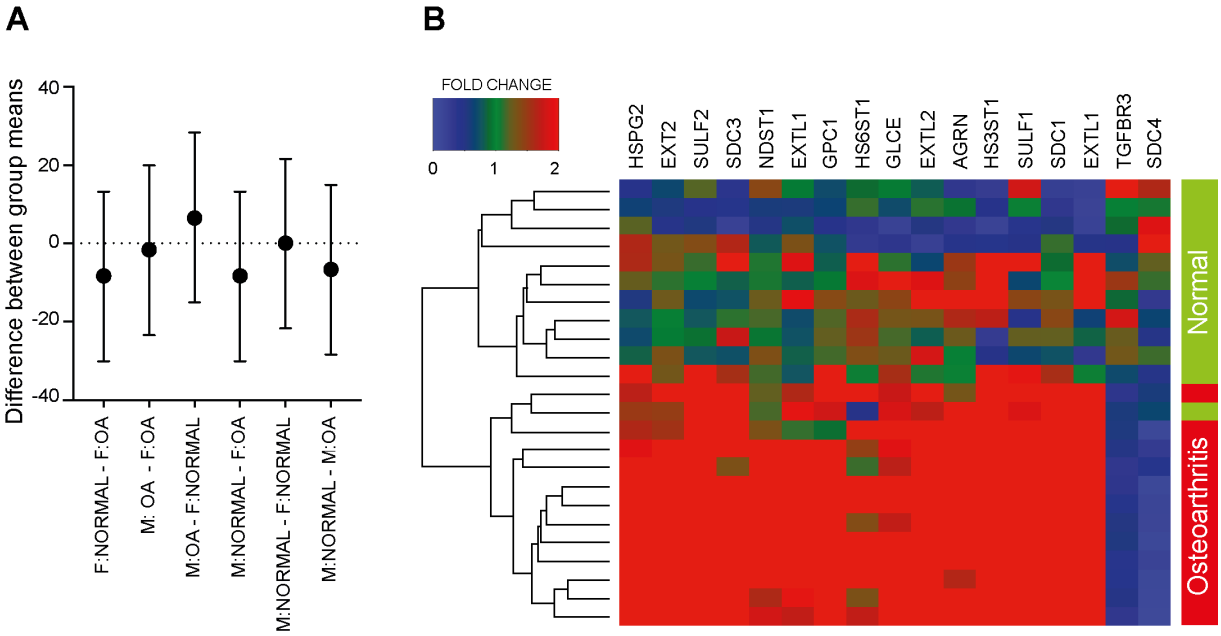

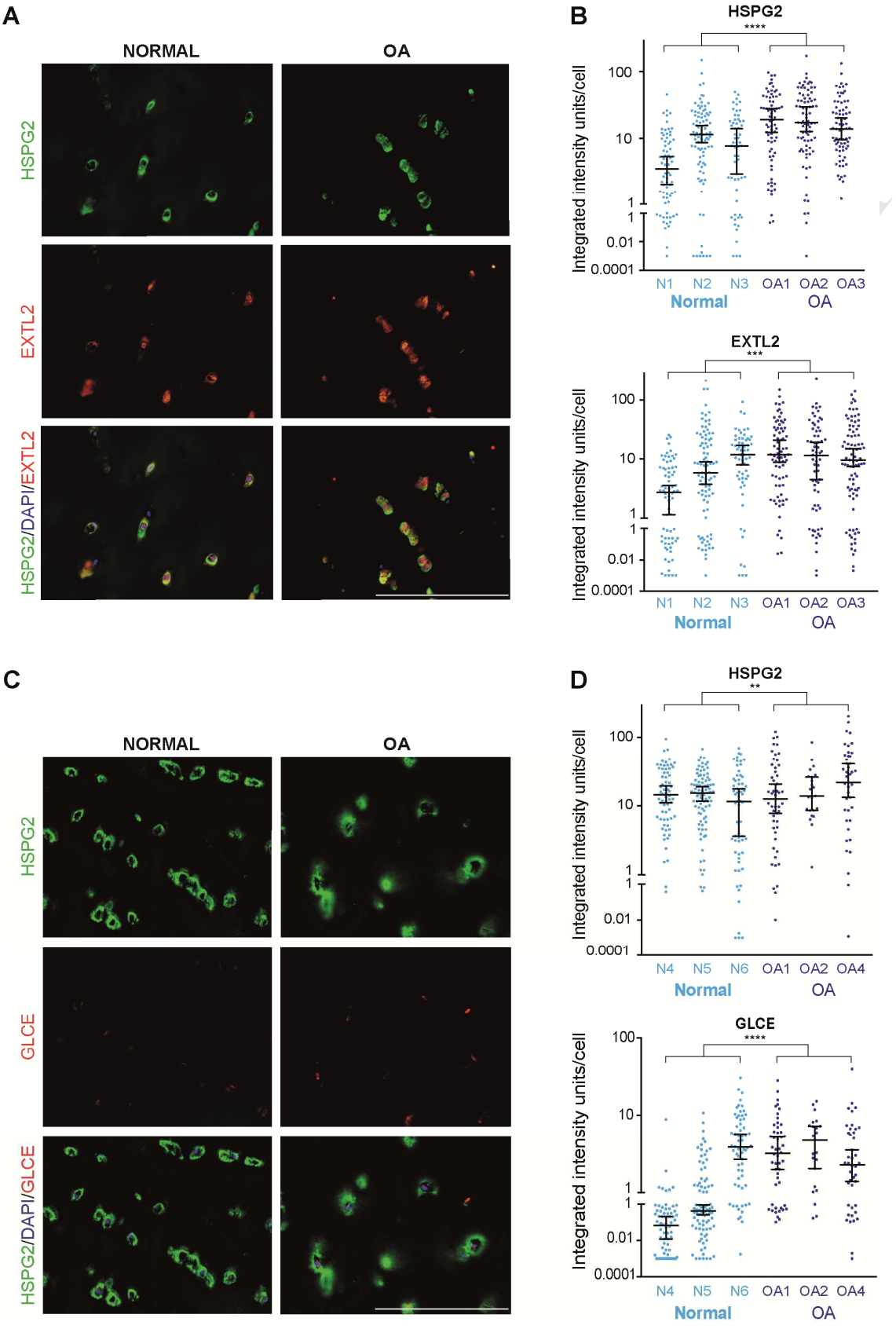
A
NORMAL
OA
HSPG2
EXTL2
HSPG2/DAPI/EXTL2
B
HSPG2
****
Integrated intensity units/cell
100
10
1
1
0.01
0.0001
N1 N2 N3 OA1 OA2 OA3
Normal
OA
EXTL2
***
Integrated intensity units/cell
100
10
1
1
0.01
0.0001
N1 N2 N3 OA1 OA2 OA3
Normal
OA
C
NORMAL
OA
HSPG2
GLCE
HSPG2/DAPI/GLCE
D
HSPG2
**
Integrated intensity units/cell
100
10
1
1
0.01
0.0001
N4 N5 N6 OA1 OA2 OA4
Normal
OA
GLCE
****
Integrated intensity units/cell
100
10
1
1
0.01
0.0001
N4 N5 N6 OA1 OA2 OA4
Normal
OA

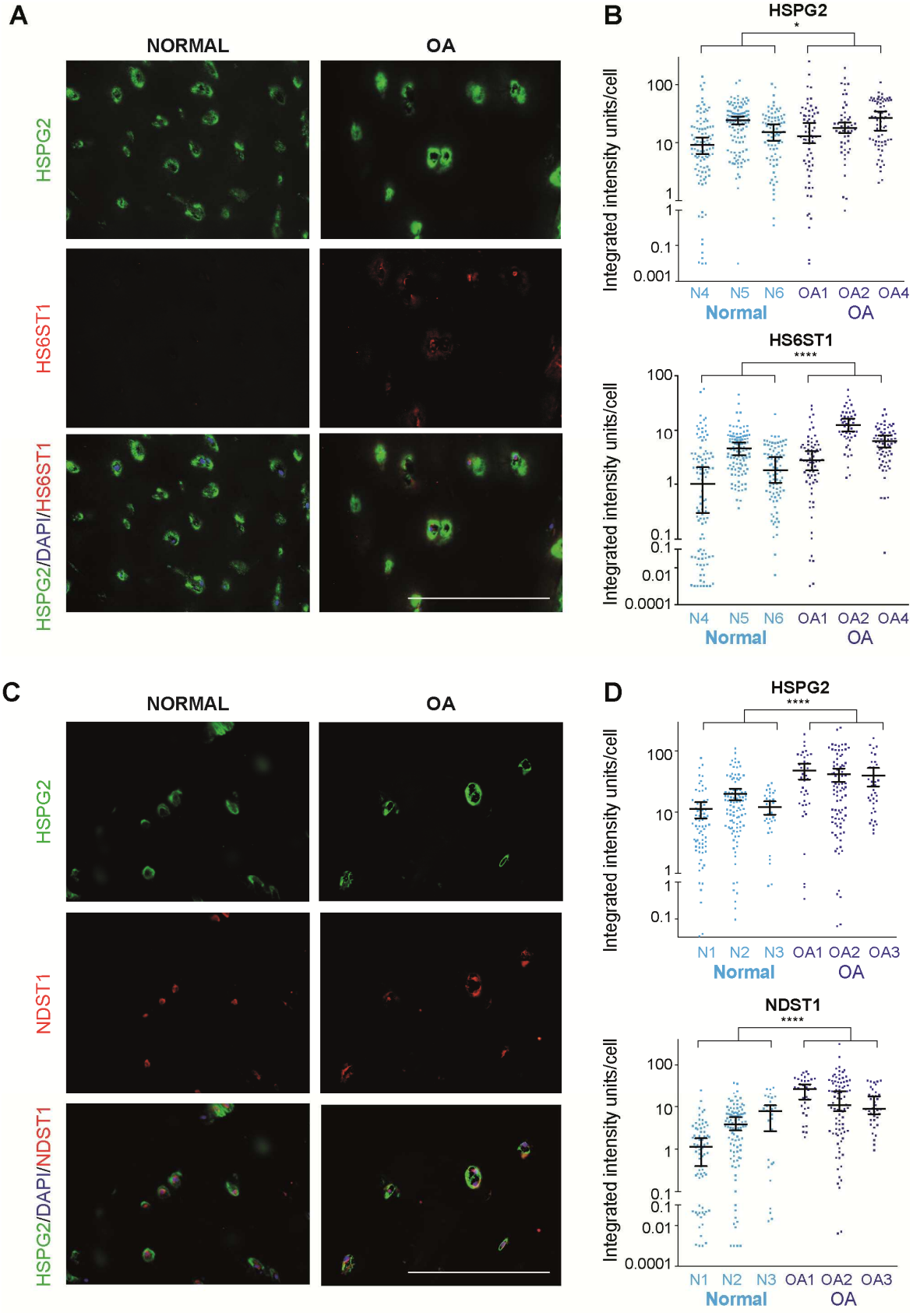
A
NORMAL
OA
HSPG2
HS6ST1
HSPG2/DAPI/HS6ST1
B
HSPG2
*
Integrated intensity units/cell
100
10
1
1
0.1
0.001
N4 N5 N6 OA1 OA2 OA4
Normal
OA
HS6ST1
****
Integrated intensity units/cell
100
10
1
0.1
0.1
0.01
0.0001
N4 N5 N6 OA1 OA2 OA4
Normal
OA
C
NORMAL
OA
HSPG2
NDST1
HSPG2/DAPI/NDST1
D
HSPG2
****
Integrated intensity units/cell
100
10
1
1
0.1
N1 N2 N3 OA1 OA2 OA3
Normal
OA
NDST1
****
Integrated intensity units/cell
100
10
1
0.1
0.1
0.01
0.0001
N1 N2 N3 OA1 OA2 OA3
Normal
OA

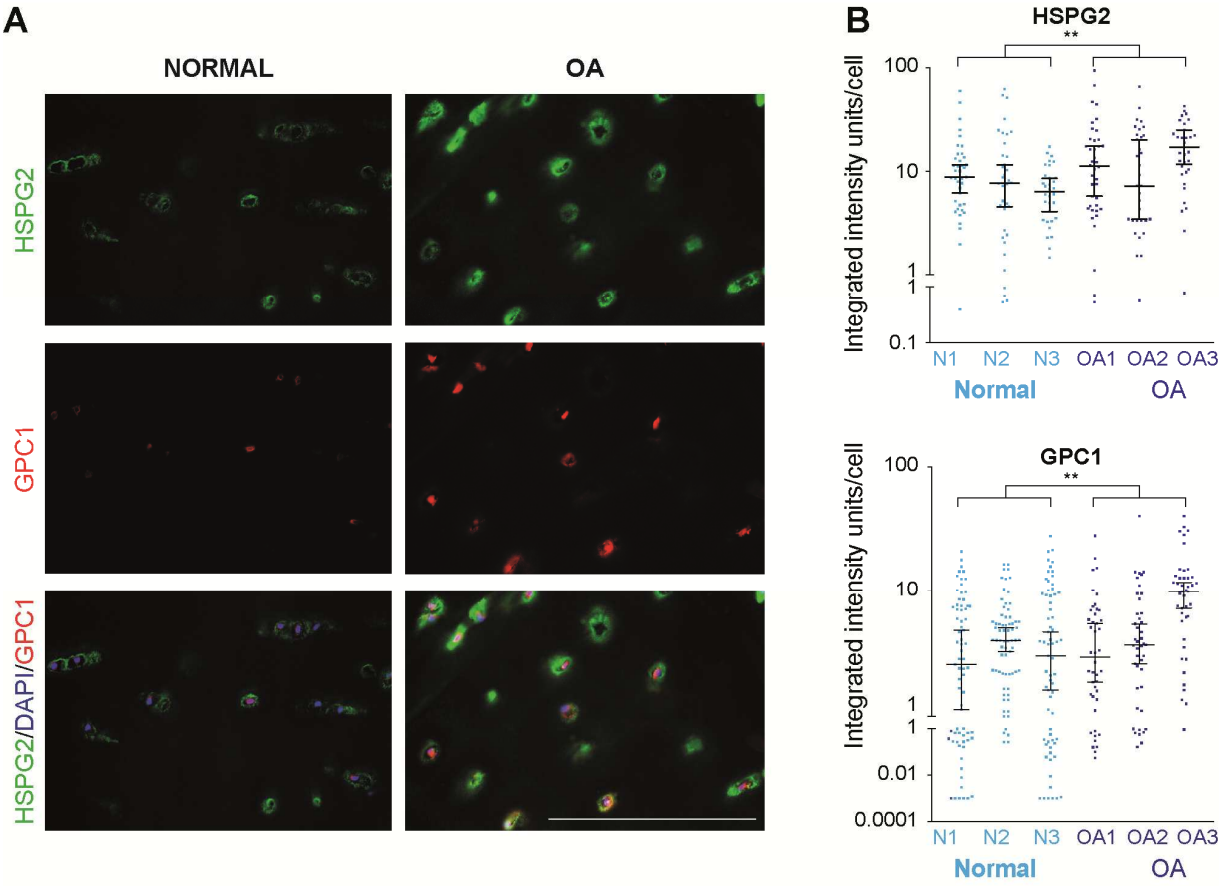
A
NORMAL
OA
HSPG2
GPC1
HSPG2/DAPI/GPC1
B
HSPG2
**
Integrated intensity units/cell
100
10
1
1
0.1
N1 N2 N3 OA1 OA2 OA3
Normal
OA
GPC1
**
Integrated intensity units/cell
100
10
1
1
0.01
0.0001
N1 N2 N3 OA1 OA2 OA3
Normal
OA

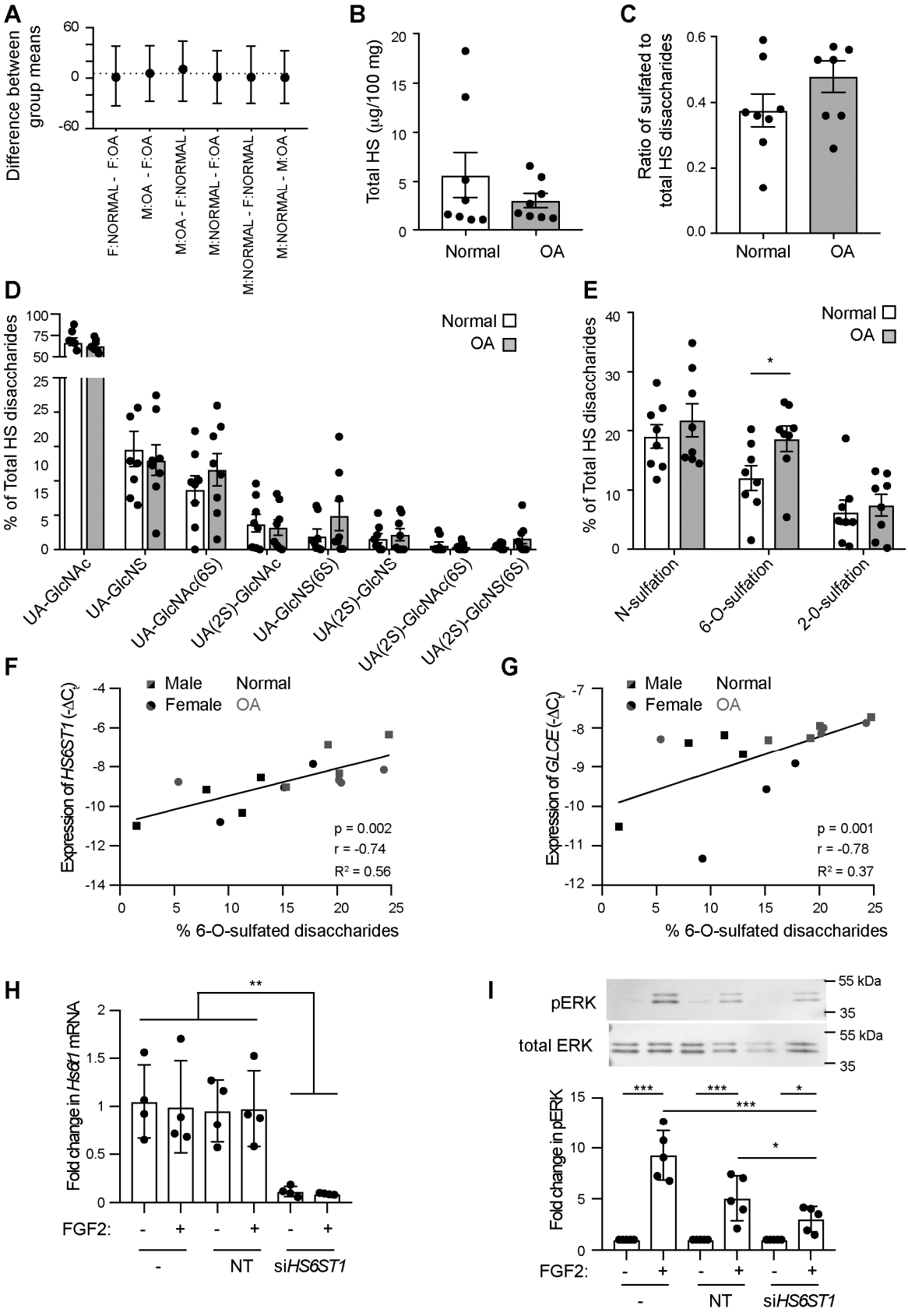
A
Difference between group means
60
0
-60
F:NORMAL - F:OA
M:OA - F:OA
M:OA - F:NORMAL
M:NORMAL - F:OA
M:NORMAL - F:NORMAL
M:NORMAL - M:OA
B
Total HS (µg/100 mg)
20
15
10
5
0
Normal
OA
C
Ratio of sulfated to total HS disaccharides
0.6
0.4
0.2
0.0
Normal
OA
D
% of Total HS disaccharides
Normal
OA
UA-GlcNAc
UA-GlcNS
UA-GlcNAc(6S)
UA(2S)-GlcNAc
UA-GlcNS(6S)
UA(2S)-GlcNS
UA(2S)-GlcNAc(6S)
UA(2S)-GlcNS(6S)
E
% of Total HS disaccharides
Normal
OA
*
N-sulfation
6-O-sulfation
2-O-sulfation
F
Expression of HS6ST1 (-ΔCt)
Male
Female
Normal
OA
p = 0.002
r = -0.74
R² = 0.56
% 6-O-sulfated disaccharides
G
Expression of GLCE (-ΔCt)
Male
Female
Normal
OA
p = 0.001
r = -0.78
R² = 0.37
% 6-O-sulfated disaccharides
H
Fold change in Hs6st1 mRNA
**
FGF2:
-
NT
siHS6ST1
I
pERK
total ERK
55 kDa
35
55 kDa
35
Fold change in pERK
***
***
*
***
*
FGF2:
-
NT
siHS6ST1